

Influence of photon-assisted energy transfer on the nonlinear refractive index of $\text{GdAlO}_3:\text{Cr}^{3+}$

E. A. Gouveia,* I. Guedes, J. C. Castro, and S. C. Zilio

Instituto de Física e Química de São Carlos, Universidade de São Paulo, Caixa Postal 369, 13560, São Carlos, São Paulo, Brazil

(Received 8 June 1992)

We have measured the nonlinear refractive index of a $\text{GdAlO}_3:\text{Cr}^{3+}$ sample as a function of light intensity and wavelength by means of the nearly degenerate two-wave mixing technique and excited-state absorption spectroscopy. It is shown that the main contribution to the nonlinear index is due to a charge-transfer transition around $45\,500\text{ cm}^{-1}$. The imaginary part of n_2 is intensity dependent and this peculiar behavior was ascribed to a photon-assisted off-resonance energy transfer between Cr^{3+} pairs.

I. INTRODUCTION

Chromium-doped materials are Kerr media that have been extensively studied during the past few years. The nature and magnitude of their nonlinear optical properties were determined mainly by means of nearly degenerate two-wave¹⁻⁵ mixing (NDTWM) and degenerate four-wave mixing⁶⁻⁸ (DFWM) techniques. It is now well established⁷ that the main contribution to the nonlinear refractive index in most of these materials comes from the large oscillator strength of charge-transfer (CT) transitions in the UV region around $50\,000\text{ cm}^{-1}$, with negligible contributions from the intermediate bands 4T_2 ($\sim 17\,000\text{ cm}^{-1}$), 4T_1 ($\sim 24\,000\text{ cm}^{-1}$), and 4T_1 (b) ($\sim 38\,000\text{ cm}^{-1}$). Among these chromium-doped media, $\text{GdAlO}_3:\text{Cr}^{3+}$ can be considered as a peculiar nonlinear optical material mainly because the Cr^{3+} ions can be added to the GdAlO_3 matrix in fairly high concentrations without any appreciable fluorescence quenching and thus, it presents a high nonlinear optical response even for samples thinner than 1 mm. Besides, NDTWM measurements have shown that the ratio (r) between the imaginary (n_2'') and real (n_2') parts of the nonlinear index ($n_2 = n_2' + in_2''$) is intensity dependent.¹ A possible explanation for this behavior could be the presence of self-diffraction of incident beams in the population grating characteristic of the TWM technique. Self-diffracted beams are easily observed in $\text{GdAlO}_3:\text{Cr}^{3+}$ and they should be taken into account when deriving the expression for the weak beam gain parameter. With this in mind, we developed a theory where the energy exchange occurring in the TWM process is regarded as the zero-order term of the intersecting beams self-diffraction in a saturated traveling grating.⁵ However, we found that the addition of self-diffracted terms does not explain the change of r with the intensity and therefore, further experimental investigation is needed in order to make this point clear.

The purpose of the present work is to investigate what sort of mechanism is responsible for the dependence of r on the intensity and for this, we used the NDTWM technique and excited-state absorption spectroscopy. The results show that the real part of the nonlinear index is in-

tensity independent and the main contribution to it comes from the charge-transfer state. We were able to estimate the cross section, frequency, and linewidth for this transition. On the other hand, the imaginary part of n_2 was found to be intensity dependent and this behavior is attributed to a photon-assisted off-resonance energy transfer (PAORET) between Cr^{3+} pairs. The PAORET process was theoretically predicted by Altarelli and Dexter⁹ in 1970 and experimentally confirmed by Duarte and Castro.¹⁰ In the present work we investigate how this process affects the nonlinear refractive index of $\text{GdAlO}_3:\text{Cr}^{3+}$.

II. EXPERIMENTS

GdAlO_3 is a crystal belonging to the space group D_{2h}^{16} , where Gd^{3+} and Al^{3+} have site symmetries C_s and C_i , respectively, and the Cr^{3+} substitutes the aluminum ion. We used a 1.4-mm-thick sample, with the c axis oriented parallel to the light propagation direction. The chromium concentration N_0 was estimated in the following way: from NDTWM experiments, which will be described later, we measured the saturation intensity at 514.5 nm ($I_s = 1.2\text{ kW/cm}^2$) and the lifetime of the 2E metastable state ($T_1 = 12\text{ ms}$). Since $I_s = \hbar\omega/\sigma_g T_1$ for the three-level system used to describe the Cr^{3+} ion,⁵ we found the absorption cross section at 514.5 nm as $\sigma_g = 2.7 \times 10^{-20}\text{ cm}^2$. Next, we measured the linear absorption coefficient ($\alpha_g = 4.2\text{ cm}^{-1}$), which allowed us to estimate $N_0 (= \alpha_g/\sigma_g)$ as $1.5 \times 10^{20}\text{ cm}^{-3}$.

In order to determine both the real and imaginary parts of n_2 , we carried out NDTWM experiments. This technique is based on the energy exchange between two light waves intersecting in the nonlinear medium.¹¹ One of the beams is much weaker than the other, with the intensity ratio being of the order of a few percent. A net energy transfer can take place whenever a phase mismatch between the interference pattern and the resulting populations grating occurs. In Kerr media, where the refractive index is intensity dependent ($n = n_0 + n_2 I$), the required phase mismatch is usually introduced by frequency shifting one of beams due to the reflection in a mirror moved by means of a piezoelectric transducer.¹²

The gain experienced by the weak beam as a function of its frequency detuning to the strong beam is given by⁵

$$\Gamma_1(\Delta) \equiv \ln \frac{I_0^-(L, \Delta)}{I_0^-(L, 0)} = \frac{4\pi n_2' L}{\lambda \cos \theta} \frac{\Delta - r \Delta^2}{1 + \Delta^2} \frac{I_0^+}{(1 + I_0^+/I_s)^2}, \quad (1)$$

where L is the sample length, $I_0^-(I_0^+)$ is the weak (strong) beam intensity, $\Delta = \Omega T_1'$, with $\Omega = \omega_+ - \omega_-$ being the frequency detuning between the strong (ω_+) and weak (ω_-) beams, $T_1' = T_1/(1 + I/I_s)$, λ is the wavelength, and 2θ is the angle between the laser beams. For $r=0$ (dispersive grating), $\Gamma_1(\Delta)$ is an antisymmetric curve. The departure from the antisymmetry indicates that an absorptive grating is also present. The fitting of the experimental points to the theoretical expression (1) allows the determination of both the real and imaginary parts of n_2 , the saturation intensity, and the lifetime T_1 of the 2E excited state.

The experimental setup, shown in Fig. 1, is similar to the one used in Ref. 2, and only a few details are presented here. The strong and weak beams are provided either by a single longitudinal mode argon-ion laser operating with a temperature-controlled intracavity étalon (operating a 514.5, 488, or 457.9 nm) or by a cw ring dye laser (1 MHz linewidth) covering the range 570–610 nm. The probe to pump intensity ratio is of the order of 1%. The frequency shift is produced by reflecting the probe beam in a mirror mounted on a piezoelectric transducer driven by a sawtooth voltage. After passing through a lens (focal length 0.6 m), the focused beams (260 μm spot size) overlap in a region where the sample is placed, making a small angle of about 2° . The transmitted pump beam is blocked while the probe beam is measured by means of a silicon photodetector.

Another technique employed, excited-state absorption spectroscopy, is important to determine the cross section involved in n_2'' . The absorption coefficient is

$$\alpha = \frac{\alpha_g + S\alpha_e}{1 + S}, \quad (2)$$

where $S = I/I_s$ is the saturation parameter and the indexes g and e stand for ground and excited states, re-

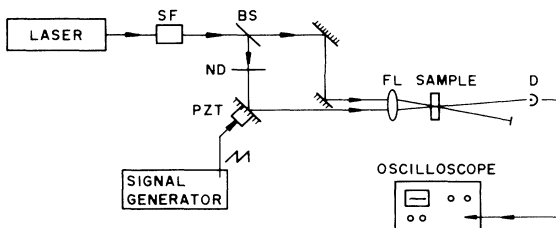


FIG. 1. Experimental setup used in nearly degenerate two-wave mixing experiment. SF: spatial filter, BS: beam splitter, ND: neutral density filter, FL: focusing lens, D: photodetector.

spectively. At low intensities ($S \ll 1$) one measures α_g , while at high intensities ($S \gg 1$) the value of α_e is obtained. The experimental procedure is the same as that used by Szabo for measurements in ruby,¹³ where, without focusing the laser beam, a low intensity is achieved and by using a lens with a short focal length, a high-intensity regime is obtained.

III. RESULTS AND DISCUSSION

Figure 2 shows the NDTWM gain in $\text{GdAlO}_3:\text{Cr}^{3+}$ as a function of detuning Δ for $\lambda = 514.5$ nm and $I_0^+(0) = 0.1$ kW/cm². The curve is not completely antisymmetric, indicating the presence of a mixed grating (dispersive/absorptive). The fitting to Eq. (1), shown by the full line in Fig. 2, provides the following values for the relevant parameters: $n_2' = 1.6 \times 10^{-7}$ cm²/W, $r = 0.09$, $T_1' = 11.2$ ms, and $I_x = 1.2$ kW/cm². An intriguing result arising from NDTWM experiments is the dependence of r on the laser intensity, which is not observed in other chromium-doped crystals, such as ruby, alexandrite, etc. This dependence is shown in Fig. 3, together with a theoretical fitting based on the PAORET process, which will be presented later. Besides, when gain curves at several intensities are analyzed by means of Eq. (1), we find that n_2' is a constant and therefore, only n_2'' is intensity dependent. This is unexpected when the usual three-level system is considered.

Referring to the real part of the nonlinear index, the parameter $(n_2' I_s)/(N_0 \lambda) = 2.4 \times 10^{-20}$ cm² is of the order of the one obtained for ruby (5.7×10^{-20} cm²), suggesting that the CT state is also responsible for the main contribution to the nonlinear index in $\text{GdAlO}_3:\text{Cr}^{3+}$. In order to verify this possibility, we carried out measurements of n_2' as a function of the wavelength, in an experiment similar to the one recently reported for ruby by Adler and Lawandy.¹⁴ The n_2' spectrum at room temperature, shown in Fig. 4, is quite smooth, except for the scattering of the data due to the experimental error, which we estimate to be between 10 and 20%. Besides, the sign of n_2' is positive in the wavelength range spanning the 4T_2 band. Assuming homogeneous broadening

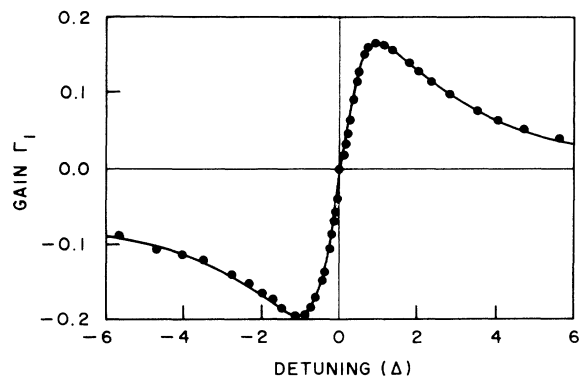


FIG. 2. Nearly degenerate two-wave mixing gain in $\text{GdAlO}_3:\text{Cr}^{3+}$ as a function of the detuning at 514.5 nm and $I_0^+ = 0.1$ kW/cm². The curve represents the best fit to the experimental data by Eq. (1).

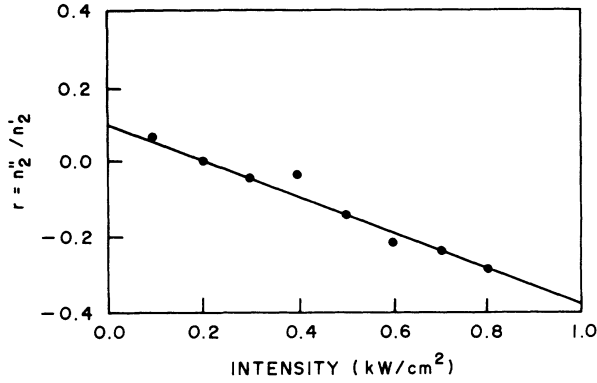


FIG. 3. Dependence of $r = n''_2/n'_2$ on the intensity of the pump beam in $\text{GdAlO}_3:\text{Cr}^{3+}$. The curve represents a theoretical fitting based on the PAORET process as explained in the text.

and that only the 4T_2 band contributes to the ground-state susceptibility, the real part of the nonlinear index can be written as

$$n'_2 = \frac{\lambda}{4\pi I_s} \left[\sum_{j>e} \frac{N_0 \sigma_{ej}^{(0)} \Delta_{ef}}{1 + \Delta_{ej}^2} - \alpha_g \Delta_{gi} \right], \quad (3)$$

where $\Delta_{ej} = [(\nu_j - \nu_e)^2 - \nu^2] / \nu \gamma_{je}$, $\Delta_{gi} \approx 2(\nu_1 - \nu) / \gamma_{gi}$, $\sigma_{ej}^{(0)}$ is the cross section at line center for a transition from the 2E excited state (e) to another excited state (j) at higher energy, γ_{je} is the linewidth for this transitions, ν_e is the energy (in cm^{-1}) of the l th level, ν is the excitation energy, and the index (i) is related to the 4T_2 band. Since the sign of n'_2 does not change on opposite sides of the 4T_2 absorption band, we conclude that the first term in Eq. (3) is always dominant, and also, Δ_{ej} must be positive. Taking into account that $\nu_e = 13\,750 \text{ cm}^{-1}$ in $\text{GdAlO}_3:\text{Cr}^{3+}$ and $\nu \approx 20\,000 \text{ cm}^{-1}$, the higher excited states are found to have an energy $\nu_j > 34\,000 \text{ cm}^{-1}$. In this spectral region there are a few sharp lines (2T_1 , 2T_2 , and 2A_2), the 4T_1 (b) band, and the CT band. The sharp lines can be immediately disregarded since they would produce sharp features in the spectrum of n'_2 . The cross

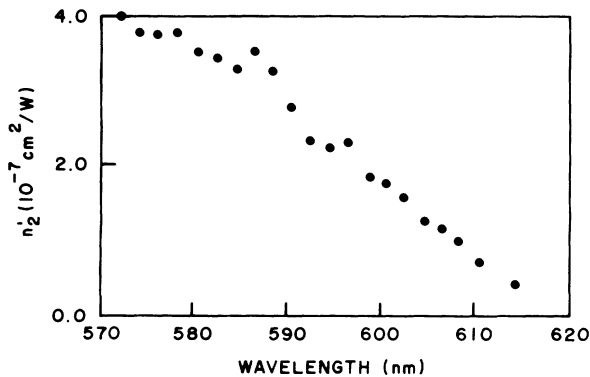


FIG. 4. Spectrum of the real part of the nonlinear index measured by means of the NDTWM technique.

section of the 4T_1 (b) band ($\sim 10^{-19} \text{ cm}^2$) is fairly small and gives rise to a value of n'_2 one order of magnitude smaller than the value measured. Therefore, the CT band seems to produce the main contribution to the nonlinear index of $\text{GdAlO}_3:\text{Cr}^{3+}$, similar to what happens in ruby.

Let us now return to the imaginary part of n_2 , which is given by

$$n''_2 = \frac{\alpha_g \lambda}{4\pi I_s} \left[1 - \frac{\sigma_e}{\sigma_g} \right], \quad (4)$$

where $\sigma_e(\sigma_g)$ is the wavelength-dependent excited (ground) state cross section. According to Fig. 3, the value of r for low intensities ($\sim 0.1 \text{ kW/cm}^2$) is around 0.09 and since $n'_2 = 1.6 \times 10^{-7} \text{ cm}^2/\text{W}$, one obtains $n''_2 \approx 1.4 \times 10^{-8} \text{ cm}^2/\text{W}$ at 514.5 nm. If we now substitute the values of α_g and I_s , we conclude that $\sigma_e \ll \sigma_g$. This is in agreement with the model based on the CT state discussed earlier. Assuming that the transition to this state gives the main contribution to n'_2 and $\Delta_{CT} \gg 1$, the value of r is obtained by taking the ratio between Eqs. (4) and (3):

$$r \approx (\sigma_g / \sigma_{CT}^{(0)}) \Delta_{CT} (1 - \sigma_e / \sigma_g). \quad (5)$$

Since $\sigma_{CT}^{(0)} = 3.3 \times 10^{-18} \text{ cm}^2$ and $\Delta_{CT} \approx 11$ (as presented below) and the value of σ_g is already known ($\sigma_g = 2.7 \times 10^{-20} \text{ cm}^2$), we find that $r \approx 0.09(1 - \sigma_e / \sigma_g)$ and therefore $\sigma_e \ll \sigma_g$.

The discussion presented above is valid in the low-intensity regime. For higher intensities, it was verified that n''_2 is a function of I and this cannot be explained by means of Eq. (4). Moreover, the experiment of excited-state absorption spectroscopy, shown in Fig. 5(a), presents an excited-state absorption larger than the ground-state one, which is the opposite of what happens at low intensities. Therefore, we conclude that Eq. (4), which is based on a three-level system, is not correct to describe our results. Thus, a new model is needed in order to explain the excited-state absorption and the mechanism we propose takes into account the PAORET process between Cr^{3+} pairs, as shown in Fig. 6. There are

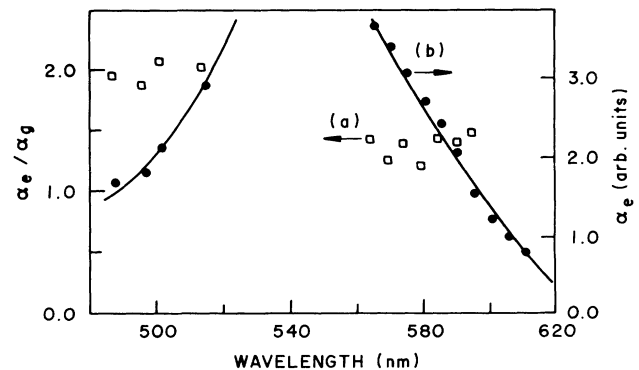


FIG. 5. (a) Ratio between the excited- and ground-state absorption coefficients (open squares) and (b) excited-state absorption spectrum (solid circles), where the full line is just for visual aid.

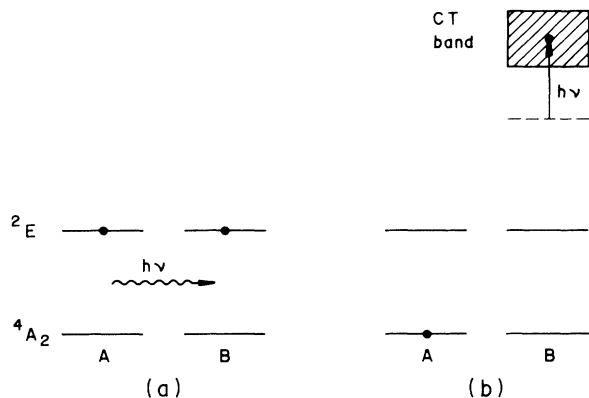


FIG. 6. PAORET process between two Cr^{3+} ions: two Cr^{3+} are in the excited state (a), and in the presence of a photon one of the ions decays to the ground state while the other one goes to the CT band (b).

initially two excited ions (A and B) nearby, and in the presence of a photon, the energy transfer occurs such that ion A ends in the ground state while ion B goes to the CT band. We tried to observe this energy transfer process by measuring the time-resolved fluorescence from the 2E level, but the fluorescence reabsorption due to the high Cr^{3+} concentration¹⁴ does not allow such a direct observation.

The absorption coefficient for the PAORET process may be written as⁹

$$\alpha_{\text{ET}}(\nu) = C_{\text{ET}} N_A N_B \sigma_A^{\text{em}} \sigma_B^{\text{ab}} \int_0^\infty g_A^{\text{em}}(\nu') g_B^{\text{ab}}(\nu' + \nu) d\nu', \quad (6)$$

where the coupling coefficient C_{ET} between two ions A and B depends on the type of the interaction (dipole, quadrupole, etc.), N_j is the j th ion concentration, σ_j is the frequency integrated cross section, g_j is the normalized line shape and the superscripts em and ab stand, respectively, for the emission ${}^2E \rightarrow {}^4A_2$ and the absorption from 2E to charge-transfer state. The emission line shape is very narrow and may be taken as $g_A^{\text{em}}(\nu') \sim \delta(\nu' - \nu_e)$, where ν_e is energy of the metastable-state fluorescence ($\nu_e = 13\,750 \text{ cm}^{-1}$). Therefore, since $N_A = N_B$, $\alpha_{\text{ET}}(\nu)$ becomes

$$\alpha_{\text{ET}}(\nu) \simeq C_{\text{ET}} N_A^2 \sigma_A^{\text{em}} \sigma_B^{\text{ab}} g_B^{\text{ab}}(\nu_e + \nu) = C_{\text{ET}} N_A^2 \sigma_A^{\text{em}} \sigma_B^{\text{ab}} [1 + 4(\nu_0 - \nu)^2 / \gamma_{\text{CT}}^2]^{-1}, \quad (7)$$

where $\nu_0 = \nu_{\text{CT}} - 2\nu_e$. At very high intensities ($S \gg 1$), $N_A = N_0 S / (1 + S) \approx N_0$ and in this case, the excited-state absorption spectroscopy will measure an ab-

sorption coefficient $\alpha_e = N_0 \sigma_e + N_0^2 F(\nu)$, with $F(\nu) = C_{\text{ET}} \sigma_A^{\text{em}} \sigma_B^{\text{ab}} g_B^{\text{ab}}(\nu_e + \nu)$. Since σ_e is small, as discussed earlier, α_e shown in Fig. 5(b) gives essentially the $F(\nu)$ function, which is proportional to the CT line shape. From this result one obtains $\gamma_{\text{CT}} \approx 3000 \text{ cm}^{-1}$ and assuming the maximum to be located around $18\,000 \text{ cm}^{-1}$, the CT band line center ν_{CT} is found to be close to $45\,500 \text{ cm}^{-1}$. With the definition of Δ_{ej} given just after Eq. (3), one finds $\Delta_{\text{CT}} \approx 11$. From Eq. (3) and the known value of n_2' at 514.5 nm , $\sigma_{\text{CT}}^{(0)}$ is found to be $3.3 \times 10^{-18} \text{ cm}^2$, which is three times smaller than in ruby.¹⁵

The absorption due to the PAORET process modifies the imaginary part of the excited-state susceptibility and consequently the imaginary part of the nonlinear index. Considering a three-level system, it is possible to show, after expanding the denominator up to first order in intensity, that n_2'' is given by

$$n_2''(I) = n_2''(0) \left[1 - \frac{F(\nu) N_0 I}{\sigma_g (1 - \sigma_e / \sigma_g) I_s} \right], \quad (8)$$

where $n_2''(0)$ is the imaginary part of the nonlinear index in the absence of the PAORET process. Therefore, r decreases linearly with I , as observed experimentally. $F(\nu)$ can be estimated from the measurement of $\alpha_e \approx N_0^2 F(\nu)$ at 514.5 nm as $F(\nu) \approx 10^{-39} \text{ cm}^5$ and so, Eq. (8) may be rewritten as

$$r(I) = r(0) [1 - 4.9I]. \quad (9)$$

Taking $r(0) \approx 0.1$, it is possible to draw the solid line in Fig. 3, which agrees well with the experimental points.

IV. CONCLUSIONS

We measured the nonlinear refractive index in $\text{GdAlO}_3:\text{Cr}^{3+}$ and verified that the main contribution to its real part comes from the CT band located at $45\,500 \text{ cm}^{-1}$, with a 3000 cm^{-1} linewidth and $\sigma_{\text{CT}} \approx 3.3 \times 10^{-18} \text{ cm}^2$ at the line center. On the other hand, the imaginary part of n_2 changes with the intensity, and this behavior was explained by taking into account the PAORET process. The off-resonant energy transfer between Cr^{3+} and Gd^{3+} in $\text{GdAlO}_3:\text{Cr}^{3+}$ was reported in Ref. 10. Although the Gd^{3+} concentration is very high ($\sim 10^{22} \text{ cm}^{-3}$), the absorption cross section ($\sigma_B^{\text{ab}} \approx 10^{-22} \text{ cm}^2$) and linewidth ($\gamma_B \approx 10 \text{ cm}^{-1}$) are small. In this context, the PAORET process between Cr^{3+} pairs is more efficient even at lower intensities because although the concentration is smaller ($\sim 10^{20}$), the cross section and linewidth of the CT bands are much larger than the absorption in Gd^{3+} .

*Permanent address: Universidade Federal de Alagoas, Cidade Universit ria, 57061, Macei , AL, Brazil.

¹J. C. Penaforte, E. A. Gouveia, and S. C. Zilio, *Opt. Lett.* **16**, 452 (1991).

²I. Mc. Michael, P. Yeh, and P. Beckwith, *Opt. Lett.* **13**, 500 (1988).

³S. A. Boothroyd, J. Chrostowski, and M. S. O'Sullivan, *J. Opt. Am. B* **6**, 766 (1986).

⁴S. A. Boothroyd, J. Chrostowski, and M. S. O'Sullivan, *Opt. Lett.* **14**, 946 (1989).

⁵S. C. Zilio, J. C. Penaforte, E. A. Gouveia, and M. J. V. Bell, *Opt. Commun.* **86**, 81 (1991).

- ⁶S. C. Weaver and S. A. Payne, *Phys. Rev. B* **40**, 10 727 (1989).
⁷R. C. Powel and S. A. Payne, *Opt. Lett.* **15**, 1233 (1990).
⁸T. Catunda and J. C. Castro, *Opt. Commun.* **63**, 185 (1987).
⁹M. Altarelli and D. L. Dexter, *Opt. Commun.* **2**, 36 (1970).
¹⁰J. L. Duarte and J. C. Castro, *Phys. Rev. B* **46**, 6578 (1992).
¹¹H. J. Eichler, P. Günter, and D. W. Pohl, in *Laser-Induced Dynamical Gratings*, edited by David L. MacAdam, *Optical Sciences Vol. 50* (Springer-Verlag, Berlin, 1986).
¹²M. A. Kramer, W. R. Tompkin, and R. W. Boyd, *Phys. Rev. A* **34**, 2026 (1986).
¹³A. Szabo, *Opt. Commun.* **12**, 366 (1974).
¹⁴C. L. Adler and N. M. Lawandy, *Opt. Commun.* **81**, 33 (1991).
¹⁵T. Kushida, *IEEE J. Quantum Electron.* **QE-2**, 524 (1966).